
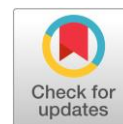


Interaction of silica with polystyrene: mechanical properties, polymer/filler adhesion and failure behavior

Selvin P. Thomas 

Department of Chemical Engineering Technology, Yanbu Industrial College, P.O. Box 30346, Yanbu Industrial City, 41912, Kingdom of Saudi Arabia

* Corresponding author: sthomas@rcjy.edu.sa



This paper belongs to a Regular Issue.

Abstract

Composites of polystyrene with different loading of silica were prepared by melt mixing in a Brabender Plasticorder at a rotor speed of 60 rpm. The mechanical properties of the composites such as tensile behavior, impact strength, and flexural properties were studied as a function of filler loading. The tensile moduli of the composites increased with silica content. To improve adhesion between the filler and the matrix, an amino silane coupling agent was used. The composites with coupling agents showed enhanced mechanical properties. Thermal properties were measured using differential scanning calorimetry (DSC), thermogravimetry (TGA) and flammability tests. Composites with 15 wt.% and 0.5 wt.% coupling agent showed optimum properties. Scanning electron microscopy (SEM) studies of the tensile fractured samples revealed the extent of filler dispersion and filler/matrix interaction. Finally, experimental results were compared with theoretical predictions.

Keywords

polystyrene
composites
mechanical properties
particulate fillers
silica
modelling

Received: 22.12.23

Revised: 19.01.24

Accepted: 19.01.24

Available online: 01.02.24

Key findings

- Silica obtained from local sources in Saudi Arabia has the potential to use as reinforcements in thermoplastics.
- Modification with silane coupling agent led to improved properties.
- Flammability of the polystyrene is decreased upon incorporation of modified silica particles.

© 2023, the Authors. This article is published in open access under the terms and conditions of the Creative Commons Attribution (CC BY) license (<http://creativecommons.org/licenses/by/4.0/>).

1. Introduction

An important attribute of polymers is the ability to modify their inherent physical properties by the addition of fillers while retaining their characteristic processing ease. Polymers can be made colored, stronger, stiffer, electronically conductive, magnetically permeable, flame retardant, harder, and more wear-resistant by the incorporation of various additives [1]. Most of these modifications are made by the addition of inorganic fillers to the polymer. These fillers, present in varying degrees, also affect the basic mechanical properties of the polymer. In many cases, the changes in the mechanical properties of the filled polymer can be predicted from basic principles [2]. In other cases, the property changes must be experimentally measured, because there is not sufficient knowledge about the polymer-

filler interactions to calculate the effect of filler concentration on property changes [3].

A polymer composite is a combined material created by the assembly of two or more components, such as a filler or reinforcing agent and a compatible matrix, to obtain specific characteristics and properties [4]. The components often offer the properties that neither constituent has. The components of a composite do not merge completely into each other but they do act in concert and are divided generally by direct boundaries. These components as well as the interface between them can usually be physically identified, and it is this behavior and properties of the interface that generally control the properties of the composite [5, 6]. The properties of a composite cannot be achieved by any of the components acting alone. To obtain the optimal properties in composites their components have to be chosen to have sharply different but complimentary properties [7, 8].

The mechanical behavior of the filled polymer systems was studied extensively [9–11]. These reports reveal that the easiest mechanical property to estimate is the modulus of the system. This is because it is a bulk property that depends primarily on the geometry, modulus, particle size distribution, and concentration of the filler. The tensile strength of a filled polymer is more difficult to predict because it depends strongly on local polymer-filler interactions as well as the above factors [12, 13]. Several investigators have shown that two general tensile strength-filler concentration responses are possible, namely the upper bound and lower bound ones [14, 15]. The upper bound response assumes strong adhesion between the polymer and filler, while the lower bound response assumes weak or no adhesion between the polymer and filler materials. Most particulate-filled polymers fall somewhere between these two responses [16, 17].

Fillers have an important role in modifying the properties of various polymers. The theory of filler reinforcement of polymers predicts the formation of a boundary layer of matrix material on the surface of the filler [18–21]. The incorporation of rigid particles substantially enhanced the stiffness of the polymer, as studied by Ahmed et al. [22]. In some cases, the filler can improve some properties while degrading others, as in Nylon-66, which has improved stiffness but reduced impact strength when filled with 30% glass [23, 24]. Recently, the effect of reinforcement of rigid particles on polymers was investigated [25, 26]. However, the particle agglomeration while preparing the composites is a great problem [27, 28]. The most important feature that affects interfacial adhesion is believed to be the mechanical stresses, chemical interactions, and physico-chemical weak boundary layers. Chemical interactions involve covalent bonding and filler/matrix wetting. Modification of the filler surface to improve adhesion has become increasingly important [29]. Strong adhesion or interfacial bond strength depends on the inherent wetting ability of the polymer and the effectiveness of the coupling agents. Incorporation of various additives or coupling agents in these systems helps to promote the adhesion at the polymer/filler interface and, hence, stress transfer between the filler and the polymer gets improved [30, 31]. Several groups are active in this area of research, and during the last decade a whole lot of fillers were introduced [32–35]. Also, several authors have made attempts to improve the mechanical and other properties of composites by modifying the surface of the filler with suitable coupling agents [36–38]. Coupling agents at fixed weight ratios have been used in the studies on HDPE/CaCO₃ composites [39, 40].

One of the most important parameters affecting the reinforcing effect of the filler is the adhesion at the interphase [18]. The polymer-filler interaction leads to the formation of localized stresses at the surface of the filler part and determine the character of the deformation and breakdown of the filled polymer [13, 41]. Fortunately, the surface chemistry of silica is much more clearly defined than that of many

other types of filler. Hence the polymer-filler interactions and their influence on the reinforcement properties of the material can be much more easily studied with silica as a filler [42, 43]. Silica can be classified, according to its nature, as natural and synthetic. Natural silica is non-reinforcing and has been used only for reducing cost [44]. The synthetic ones are reinforcing and nowadays have particle sizes as small as the carbon blacks besides an extremely reactive surface [45]. Silica can also be classified, according to the production method, into three groups: pyrogenic silica, obtained by high-temperature processes (thermal or electrical), silica gel, and precipitated silica. Silica obtained by high-temperature processes has a very high cost. Silica obtained by precipitation has a lower cost and has been more frequently used as a reinforcing filler. Therefore, the latter was chosen for the present study. The silica micro particles were locally produced in Saudi Arabia and were generously donated to study the reinforcing capabilities. The particles were white and were expected to have good dispersion properties. To improve the dispersion, the surface of the particles was treated with a silane-based coupling agent, 3-aminopropyl trimethoxy silane. The goal of the present study is to establish the reinforcing characteristics of silica-filled polystyrene composites. The effect of the coupling agent on the filler matrix interaction is also studied.

2. Materials and methods

2.1. Materials

The polymer used for the study is atactic polystyrene. It was obtained from Polychem Limited, Bombay, India. The specific properties of the used polymer are: density 1.04 g/cm³, Poisson's ratio 0.333, water absorption 0.05%, softening temperature 108 °C and molecular weight of 218000. Silica was obtained from Saudi Geological Survey, Jeddah, and its properties are: density 1.64 g/cm³, average particle diameter 167 μm, specific gravity 4.1, pH in the range of 6–8. 3-aminopropyl trimethoxy silane (APTMS) was obtained from Fischer scientific USA.

2.2. Preparation of composites

Polystyrene/silica micro composites were prepared in a Brabender Plasticorder (Brabender, Germany) at a rotor speed of 60 rpm for 8 min at a temperature of 180 °C. The compositions of the fillers were 0, 5, 10, 15, 20, and 25% by weight, and the samples were labelled as S0, S5 and so on. Based on the optimum properties of the composites, one of the composites was selected for filler modification. To enhance the filler/matrix adhesion, a silane-based coupling agent, 3-aminopropyl trimethoxy silane, was used. The silica particles were first heated in an oven at 90 °C for 6 h to remove the moisture and then mixed with 0.1, 0.3, 0.5, 0.7, and 1 weight ratio of the coupling agent. They were mixed in the Brabender Plasticorder with polystyrene with 10 wt.% silica. After optimization of the amount of coupling agent as 0.5 wt.%,

composites were prepared with up to 25 wt.% of modified silica, and they were labelled as Co, C5 and so on. The composites were made into sheets using a hydraulic press at a pressure of 200 kg/cm² at 180 °C. Rectangular samples of 10×1.2×0.2 cm³ were cut for tensile testing, 6×1.2×0.2 cm³ for impact testing and 12×1.2×0.2 cm³ for flexural studies.

2.3. Characterization techniques

Tensile and flexural measurements were carried out using a Universal Testing Machine (TNE 400 series) at a cross-head speed of 10 mm/min at room temperature. From the stress-strain curves, the tensile strength, Young's modulus, and elongation at break of the composites were determined. The tensile properties were determined according to ASTM D638. Izod Impact testing was done in an ITS AMP 105 impact tester. The impact strength was determined by striking the bar-shaped specimen with a hammer as per ASTM D256. The flexural properties were determined by applying the three-point bending load to a rectangular specimen (ASTM D 790), which rested on a block at both ends.

Thermogravimetric analysis (TGA) was carried out in a Shimadzu TA60 DTG analyzer in nitrogen atmosphere. Thermograms were obtained from room temperature to 700 °C at a heating rate of 10 °C min⁻¹. Thermal analysis was carried out using a differential scanning calorimetry (DSC) on a pyris1 DSC (PerkinElmer, USA). Nitrogen gas at a rate of 70 mL min⁻¹ was used as purging gas. Aluminum pans containing 2–3 mg of the samples was heated from room temperature to 200 °C at a heating rate of 10 °C min⁻¹.

Small-scale flammability tests were carried out on the Federal Aviation Administration's Pyrolysis Combustion Flow Calorimeter, and the samples were tested in triplicate according to ASTM D7309-07 with the samples of 5±0.5 mg in weight. The heating rate was 60 °C/min in an 80 cm³/min stream of nitrogen; the maximum pyrolysis temperature was 900 °C. The anaerobic thermal degradation products in the nitrogen gas stream were mixed with a 20 cm³/min stream of oxygen prior to entering the combustion furnace at 900 °C. The heat release was determined by oxygen consumption calorimetry. Peak heat release rate (PHRR) data were reproducible within ±0.5%. The Scanning electron Microscopy studies of the fractured samples were done using a JEOL 840 S microscope.

3. Results and discussion

3.1. Stress-strain behaviour in tension

Figures 1 and 2 show the stress-strain curves of the composites of polystyrene and silica. Figure 1 demonstrates the stress-strain curves of polystyrene with silica in different weight percentages. The pure polymer and filled composites show typical stress-strain curves similar to the brittle polymers. From the initial linear part of the curve, modulus properties can be measured. The filler addition improved the moduli.

Figure 2 shows the stress strain curves of the polystyrene composites with varying amounts of silica particles

with 0.5 wt.% of the coupling agent. The brittle nature of the composites is still prevailing; however, the moduli and ultimate break regions improved on account of the better interaction between the filler and the matrix. The modification of the interfacial bond between the filler and the matrix led to the improvement in stress-strain behavior, as evidenced by Maldas et al. [46]. An interesting study related to the modification of silica micropowder and its usage as a filler in PVC polymer was reported recently [47]. The authors mentioned that the modification to the silica micropowder improved the dispersion in the polymer matrix, thereby improved tensile strength, flexural strength and notched impact strength significantly.

3.2. Young's modulus

The Young's moduli of the composites were obtained from the stress-strain plots. Young's modulus usually increases for a polymer when fillers are added to it due to the higher inherent modulus of the filler compared to the polymer matrix [48]. Figure 3 shows the behavior of Young's modulus of polystyrene with respect to silica loading with and without coupling agent.

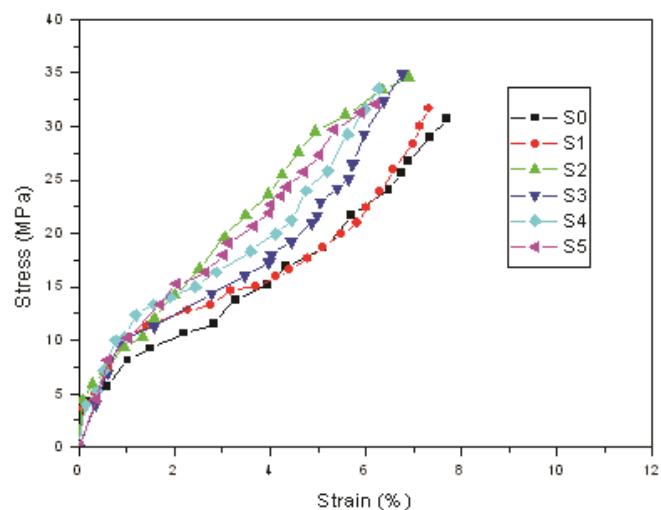


Figure 1 Stress strain behavior of the silica filled polystyrene composites without coupling agent.

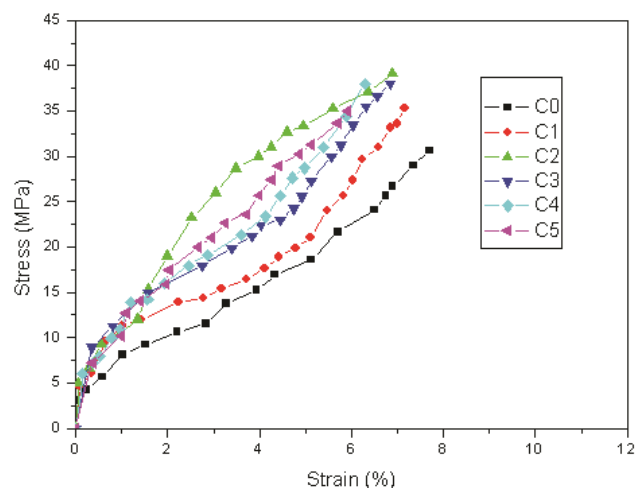


Figure 2 Stress strain behavior of the silica filled polystyrene composites with 0.5 wt.% of coupling agent.

As can be seen from Figure 3, the modulus values increase with filler loading for both systems. The silane treated composites have higher Young's modulus due to the better interfacial interaction between the filler and the matrix. The increase in modulus can be ascribed to the aspect ratio of the filler, the orientation of the fillers, interfacial interaction, and the nature of the failure [49-51].

3.3. Tensile strength

Figure 4 shows the changes in tensile strength of the composites with and without the coupling agent. Tensile strength increases for the composites up to 10 wt.% of silica for both cases, and thereafter the values are decreasing due to the agglomeration of the fillers in the matrix. The increment in tensile strength for the coupling agent added systems can be attributed to the better interaction between the filler and the matrix. Silane coupling agent improved the interphase between filler and the polystyrene matrix. In order to understand the effect of coupling agent on the tensile properties, 10 wt.% silica with varying coupling agent loaded composites were utilized to plot Young's modulus and the tensile strength (Figure 5). The optimum concentration for the coupling agent is 0.5 wt.% as evidenced from the figure.

3.4. Flexural studies

Flexural properties are very important for the composites to understand the load bearing capacity. Figure 6 shows the effect of silica on the flexural modulus of the polystyrene composites. The maximum value of flexural modulus is given by 15 wt.% of silica reinforced polystyrene composites. In the case of flexural strength, the maximum is obtained for composites having 10 wt.% of filler (Figure 7). There is appreciable improvement in the modulus and strength for the composites with coupling agent treated silica. The interaction with filler and matrix makes the composites more stable against the flexural force. As in the case of tensile strength, beyond 15 wt.% of the filler loading the flexural property decreases due to particle agglomeration.

3.5. Theoretical modelling

Filler dispersion, orientation, shape and their ability to adhere to the matrix and several other parameters contribute to the improvement in mechanical properties. Theoretically, one can predict the mechanical characteristics taking into account these parameters.

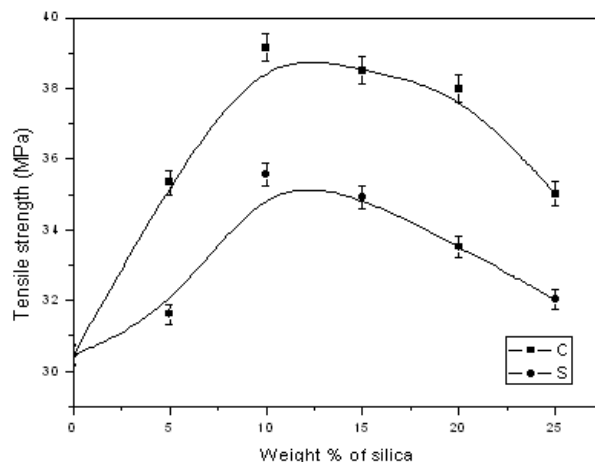


Figure 4 Tensile strength of the silica filled polystyrene composites with and without the coupling agent.

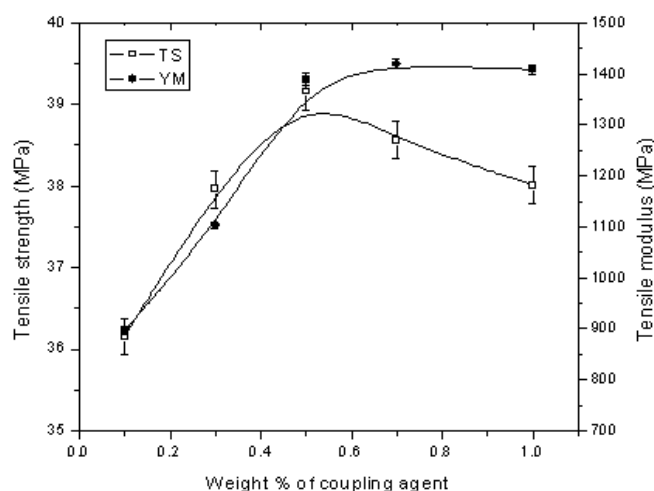


Figure 5 Effect of coupling agent on the tensile strength and Young's modulus of the composites.

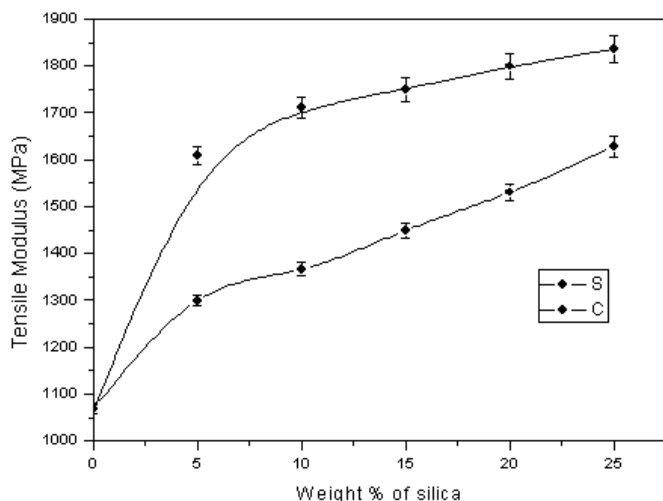


Figure 3 Young's Modulus of the silica filled polystyrene composites with and without the coupling agent.

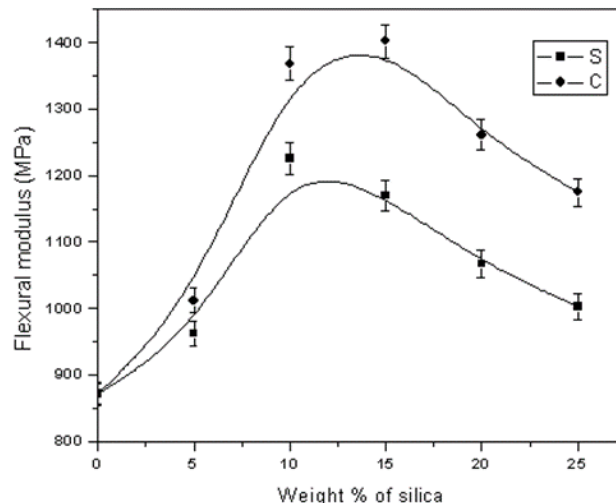


Figure 6 Flexural modulus of the silica filled polystyrene composites with and without the coupling agent.

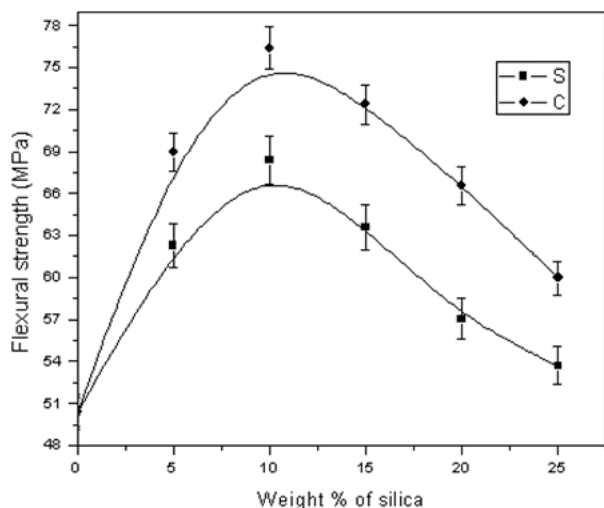


Figure 7 Flexural strength of the silica filled polystyrene composites with and without the coupling agent.

There are several theories for predicting mechanical properties available nowadays. Most of the theories depend on the matrix properties and the filler properties. The important theories are developed by Einstein, Guth, Mooney, Kerner, Thomas and Nielson [48, 52, 53].

3.5.1. Einstein equation

Einstein and Guth equations are mainly used for the theoretical calculations of the properties of composites with spherical (particulate) fillers. According to Einstein's equation, for a rigid filler and the matrix,

$$M_c = M_m(1 + 1.25V_p), \tag{1}$$

where M_c and M_m are Young's modulus of composite and matrix, respectively, and V_p is the particle volume fraction. Einstein's equation is applicable only for materials filled with low concentrations of non-interactive spheres. This equation shows that the volume occupied by the filler is independent of the size of the filler particles, which is the prominent variable for modulus of the composites.

3.5.2. Guth equation

$$M_c = M_m(1 + 1.25V_p) + 14.1V_p^2, \tag{2}$$

Guth's equation is an extension of Einstein's equation that takes into consideration the inter-particle interactions at higher filler concentrations.

3.5.3. Kerner equation

Young's modulus of spherically shaped particulate-filled polymer composites is given by Kerner's equation

$$M_c = M_m \left[1 + \frac{15V_p(1 - \sigma_m)}{V_m(8 - 10\sigma_m)} \right], \tag{3}$$

where V_m is the matrix volume fraction and σ_m is the Poisson's ratio of the matrix.

3.5.4. Quemeda equation

$$M_c = M_m \frac{1}{(1 - 0.5KV_p)^2}, \tag{4}$$

where K is a constant typically equal to 2.5. This variable coefficient is introduced to account for the inter-particle interactions and differences in particle geometry.

3.5.5. Thomas equation

$$M_c = M_m(1 + 2.5V_p + 10.05V_p^2 + 0.00273exp[16.6V_p]). \tag{5}$$

Thomas equation is an empirical relationship based on the data generated with dispersed spherical particles.

These theoretical predictions (3.5.1-3.5.5) were plotted with the experimental result in Figure 8. At lower filler loading the experimental data agree with Quemeda (at 0.12 volume fraction) and Guth (0.07 volume fraction) models. The experimental results agree with Einstein and Kerner's equations at a higher volume fraction of filler. The modulus values increase upon adding the fillers into the system. Einstein's equation predicts an increase in modulus for increased filler amounts, and the experimental result agrees with it.

3.6. Impact properties

Apart from the polymer-filler adhesion, other adhesive forces also affect the impact properties of the filled polymers [54]. The fracture mechanism of the polymer in the filled and unfilled states are different, which can lead to improvement in impact properties. Generally, the impact properties of the filled system are lower than the unfilled system in case there is good filler/matrix interaction [55].

The impact energy of the composites is shown in Figure 9. The impact energy shows a decreasing trend with respect to filler loading. Comparing the filled systems with and without coupling agents, the coupling agent added systems have higher impact energy in all compositions due to the better filler/matrix adhesion. In the presence of the coupling agent, the interfacial bonding between the matrix and the filler increases and thus facilitates better transfer of stress.

3.7. Thermal properties

TGA was used to measure the thermal stability of the composites in the temperature range of 30–700 °C. The representative thermograms of the coupling agent modified silica reinforced composites are given in Figure 10. The thermal properties of the composites are given in Table 1.

According to the data, the thermal stability of polystyrene is lower than that of the composites. This is due to high thermal stability of the modified silica particles in the system.

Table 1 DSC and TGA characteristics of polystyrene composites with the coupling agent.

Compo-sites	DSC (°C)	Wt.% remaining at different temp. (TGA)		TGA characteristics (°C)		
		350 °C	500 °C	T_{10}	T_{50}	T_{max}
Co	100.5	87.9	0.5	344	371	375.8
C1	102	90.7	9.6	357	382	383.8
C3	103.8	88.0	14.8	343	381	390.8
C5	101	87.4	29.7	329	364	381.8

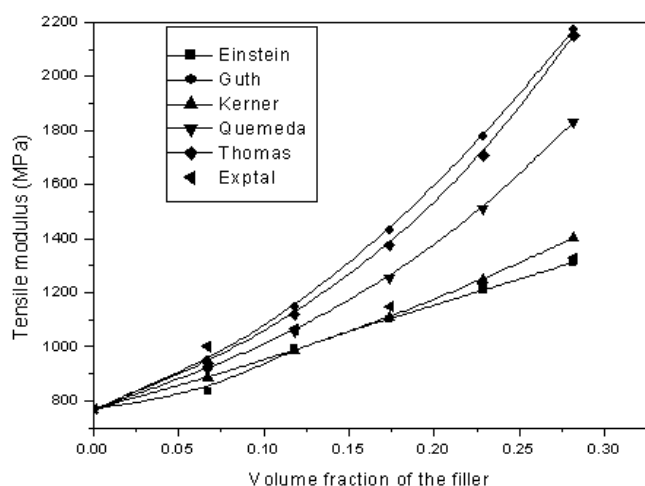


Figure 8 Theoretical modelling of the tensile moduli of silica filled polystyrene composites.

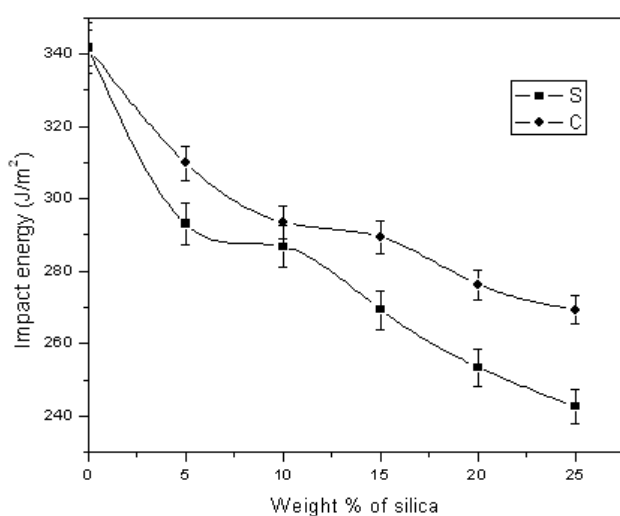


Figure 9 Impact strength of the silica filled polystyrene composites with and without the coupling agent.

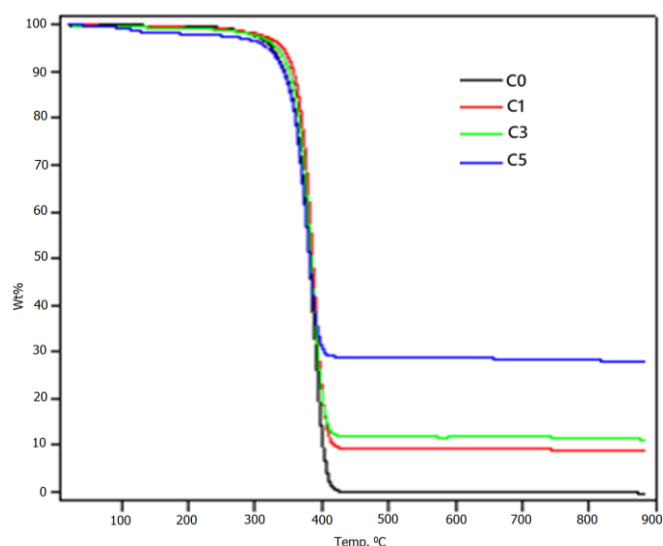


Figure 10 TGA curves of the silica filled polystyrene composites with the coupling agent.

Physical interaction between the surface of the silica particles and the polystyrene chains is one of the important factors for improving the thermal stability of the polymer

matrix. Table 1 also shows the glass transition temperature (T_g) of the polystyrene composites with modified silica particles. It can be seen that the pure polystyrene has lower T_g than the composites. The rigid particles of silica can restrict the steric movement of the polystyrene chains and induce inflection in the DSC measurements at higher temperatures. Glass transition temperature of polystyrene with unmodified silica particles showed little change. The pure PS showed a T_g of 100 °C, and the incorporation of silica particles increased the T_g values by 0.5–1 °C. So, these results were not included in Table 1. The increase in T_g is marginal and amounts to 2–3 °C for all the composites with silica modified with coupling agent.

A pyrolysis combustion flow calorimeter, also known as a microscale combustion calorimeter (MCC) was utilized to measure the flammability of the samples. The parameters obtained by MCC are heat release capacity (HRC), peak heat release rate (PHRR), total heat release (THR), and reduct-MCC, which are presented in Table 2.

HRC is the ratio of the maximum heat release rate to constant heating rate which helps one to understand the fire hazard of a material. As can be seen from Table 2, the HRC was found to decrease with the increase in silica loading due to the good dispersion of the filler in the matrix. The thermal conductivity of the filler is greater than that of the polymer matrix which assists in conducting the heat throughout the polymer matrix. As evidenced from Table 2, when the filler loading was increased to 25%, HRC values dropped to 22% compared to the polymer without filler.

Another important parameter to measure the fire hazard is HRR. The reduction in PHRR is very important with respect to the fire safety aspects of a material. PHRR indicates the point at which the fire will propagate further or adjacent objects might be ignited. It is obvious that the addition of modified silica filler reduced PHRR and this reduction is propagated with respect to filler loading. For 25 wt.% of filler loading the PHRR value decreased by almost 28%. However, the total heat release, which is the integral of the HRR curve over the duration of the experiment, decreases marginally with filler loading.

Reduct-MCC (%) is the percent deduction in PHRR of the composites with respect to pure PS. The mechanism of reduction in the flammability properties of the PS composites may be attributed to the barrier effect of the silica filler, which inhibited the emission of degraded gas molecules and prevented the oxygen supply from reaching the surface.

Table 2 Flammability properties of polystyrene composites with the coupling agent.

Sample	HRC (J/gK)	PHRR (W/g)	THR (kJ/g)	Reduct-MCC (%)
C0	1119±7	1300±8	38.58±0.2	-
C1	979±6	1123±6	36.03±0.5	7
C3	912±4	1009±5	35.49±0.7	19
C5	883±5	951±6	31.12±0.1	29

3.8. Scanning electron microscopy studies

Scanning electron microscopy (SEM) images of the tensile fractured samples of composites are given in Figures 11 and 12. The silica particles are shown in the SEM images in the red circled areas. From Figure 11 it can be seen that low loading of silica without coupling agent has good dispersion, which get agglomerated at higher loading ($\geq 15\%$). This accounts for the decrease of properties at higher filler loading. Figure 12 shows the fracture surface of composites containing coupling agents. Even though agglomeration is seen at higher loadings, the coupling agent-containing system shows good dispersion and improved filler/matrix interface adhesion as compared to the system with no coupling agent.

4. Limitations

The composites were prepared using solvent free fabrication technique, but the filler dispersion is a problem on account of the agglomeration at higher loadings. The modification of the silica particles with silane coupling agent leads to improved properties, and the samples with higher loading becomes brittle due to the nature of the thermo-plastic characteristics. An impact modifier could be added so that the properties could be even more improved. However, achieving better dispersion in the matrix will be challenging.

5. Conclusions

Polystyrene samples with silica with and without modification were studied in this work. The mechanical properties such as Young's modulus, tensile strength, flexural modulus, and flexural strength increase linearly with the increase in the filler concentration followed by a decrease beyond 15 wt.%. The decrease at higher loading is due to the particle-particle interaction leading to agglomeration. The system containing coupling agents reduced the agglomeration considerably, and the properties were improved significantly due to better interaction between filler and matrix. As expected, the impact properties of the composites decreased with filler content due to the brittle nature of the matrix. The thermal properties and flammability properties also showed appreciable improvement. The scanning electron microscopy studies indicated that at lower loading silica is well dispersed in the PS matrix, but at higher loading the silica agglomerates. Finally, the experimental results were compared with theoretical predictions. At lower filler loading the experiment results agree with Quemada (at 0.12 volume fraction) and Guth (at 0.07 volume fraction) models, and at higher volume fraction of filler the experimental results agree with Einstein and Kerner equations.

• Supplementary materials

No supplementary materials are available.

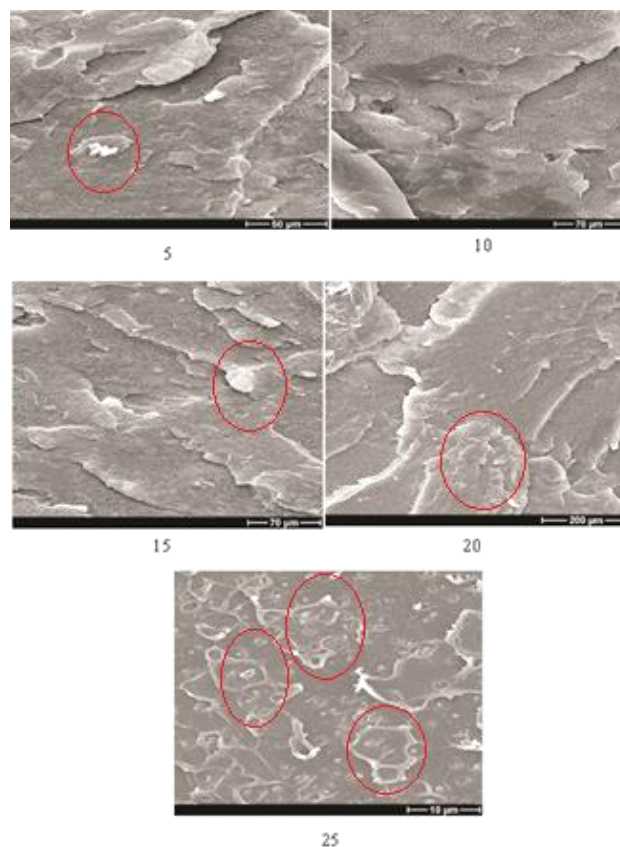


Figure 11 SEM images of the tensile fractured samples of the composites without the coupling agent.

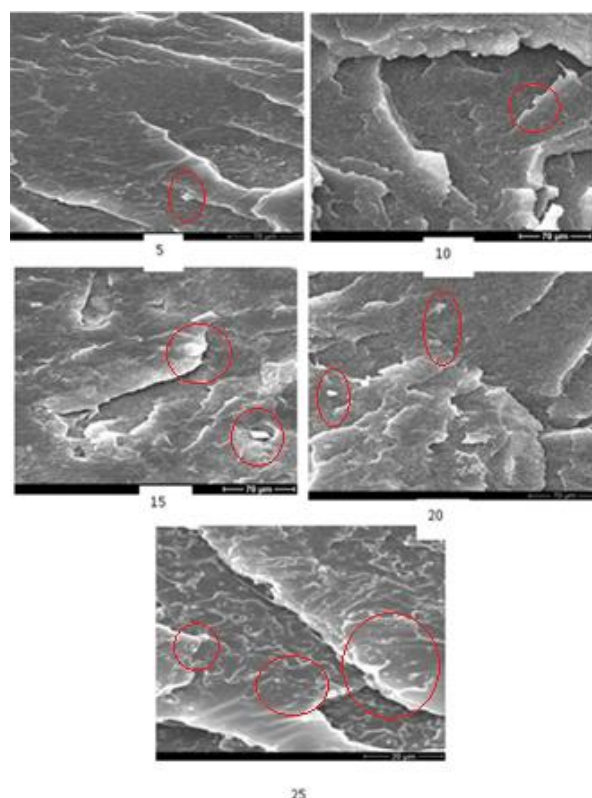


Figure 12 SEM images of the tensile fractured samples of the composites with the coupling agent.

• Funding

This research had no external funding.

● Acknowledgments

None.

● Author contributions

The Author prepared this article by himself, including the conceptualization, data curation, formal analysis, investigation, writing, editing, and finishing.

● Conflict of interest

The author declares no conflict of interest.

● Additional information

Author ID:

Selvin P. Thomas, Scopus ID [55456106400](https://orcid.org/0009-0001-5545-6106).

Website:

Yanbu Industrial College, <http://www.rcyci.edu.sa/en/yic/>.

References

- Ramakoti IS, Panda AK, Gouda N. A brief review on polymer nanocomposites: current trends and prospects. *J Polym Eng.* 2023;43:651–679. doi:[10.1515/polyeng-2023-0103](https://doi.org/10.1515/polyeng-2023-0103)
- Teimouri A, Barbaz Isfahani R, Saber-Samandari S, Salehi M. Experimental and numerical investigation on the effect of core-shell microcapsule sizes on mechanical properties of microcapsule-based polymers. *J Compos Mater.* 2022;56:2879–2894. doi:[10.1177/00219983221107831](https://doi.org/10.1177/00219983221107831)
- Łapińska A, Grochowska N, Antonowicz J, Michalski P, Dydek K, Dużyńska A, Daniszewska A, Ojrzyńska M, Zeranska K, Zdrojek M. Influence of the filler distribution on PDMS-graphene based nanocomposites selected properties. *Sci Rep.* 2022;12(1):19038. doi:[10.1038/s41598-022-23735-3](https://doi.org/10.1038/s41598-022-23735-3)
- Mishra T, Mandal P, Rout AK, Sahoo D. A state-of-the-art review on potential applications of natural fiber-reinforced polymer composite filled with inorganic nanoparticle. *Compos Part C Open Access.* 2022;9:100298. doi:[10.1016/j.jcomc.2022.100298](https://doi.org/10.1016/j.jcomc.2022.100298)
- Agustiany EA, Rasyidur Ridho M, Rahmi DN M, Madyaratri EW, Falah F, Lubis MA, Solihat NN, Syamani FA, Karungamye P, Sohail A, Nawawi DS. Recent developments in lignin modification and its application in lignin-based green composites: A review. *Polym Compos.* 2022;43:4848–4865. doi:[10.1002/pc.26824](https://doi.org/10.1002/pc.26824)
- Ravindran L, MS Sreekala, Kumar S A, Thomas S. A comprehensive review on phenol-formaldehyde resin-based composites and foams. *Polym Compos.* 2022;43:8602–8621. doi:[10.1002/pc.27059](https://doi.org/10.1002/pc.27059)
- Rajak DK, Wagh PH, Linul E. A review on synthetic fibers for polymer matrix composites: performance, failure modes and applications. *Mater.* 2022;15:4790. doi:[10.3390/ma15144790](https://doi.org/10.3390/ma15144790)
- Jagadeesh P, Puttegowda M, Rangappa SM, Alexey K, Gorbatyuk S, Khan A, Doddamani M, Siengchin S. A comprehensive review on 3D printing advancements in polymer composites: technologies, materials, and applications. *Int J Adv Manuf Technol.* 2022;121:127–169. doi:[10.1007/s00170-022-09406-7](https://doi.org/10.1007/s00170-022-09406-7)
- Zare Y. Study of nanoparticles aggregation/agglomeration in polymer particulate nanocomposites by mechanical properties. *Compos Part A Appl Sci Manufact.* 2016;84:158–164. doi:[10.1016/j.compositesa.2016.01.020](https://doi.org/10.1016/j.compositesa.2016.01.020)
- Popescu D, Zapciu A, Amza C, Baciu F, Marinescu R. FDM process parameters influence over the mechanical properties of polymer specimens: A review. *Polym Test.* 2018;69:157–166. doi:[10.1016/j.polymertesting.2018.05.020](https://doi.org/10.1016/j.polymertesting.2018.05.020)
- Alsubari S, Zuhri MY, Sapuan SM, Ishak MR, Ilyas RA, Asyraf MR. Potential of natural fiber reinforced polymer composites in sandwich structures: A review on its mechanical properties. *Polymers.* 2021;13:423. doi:[10.3390/polym13030423](https://doi.org/10.3390/polym13030423)
- Song Y, Zheng Q. Concepts and conflicts in nanoparticles reinforcement to polymers beyond hydrodynamics. *Progr Mater Sci.* 2016;84:1–58. doi:[10.1016/j.pmatsci.2016.09.002](https://doi.org/10.1016/j.pmatsci.2016.09.002)
- Plagge J, Lang A. Filler-polymer interaction investigated using graphitized carbon blacks: Another attempt to explain reinforcement. *Polymer.* 2021;218:123513. doi:[10.1016/j.polymer.2021.123513](https://doi.org/10.1016/j.polymer.2021.123513)
- Siraj S, Al-Marzouqi AH, Iqbal MZ, Ahmed W. Impact of micro silica filler particle size on mechanical properties of polymeric based composite material. *Polymers.* 2022;14:4830. doi:[10.3390/polym14224830](https://doi.org/10.3390/polym14224830)
- Meddad A, Fisa B. Stress-strain behavior and tensile dilatometry of glass bead-filled polypropylene and polyamide 6. *J Appl Polym Sci.* 1997;64:653–65. doi:[10.1002/\(SICI\)1097-4628\(19970425\)64:4<653::AID-APP4>3.0.CO;2-M](https://doi.org/10.1002/(SICI)1097-4628(19970425)64:4<653::AID-APP4>3.0.CO;2-M)
- Bartczak Z, Argon AS, Cohen RE, Kowalewski T. The morphology and orientation of polyethylene in films of sub-micron thickness crystallized in contact with calcite and rubber substrates. *Polymer.* 1999;40:2367–2380. doi:[10.1016/S0032-3861\(98\)00443-1](https://doi.org/10.1016/S0032-3861(98)00443-1)
- Liu ZH, Kwok KW, Li RK, Choy CL. Effects of coupling agent and morphology on the impact strength of high density polyethylene/CaCO₃ composites. *Polymer.* 2002;43:2501–2506. doi:[10.1016/S0032-3861\(02\)00048-4](https://doi.org/10.1016/S0032-3861(02)00048-4)
- Idumah CI, Obele CM. Understanding interfacial influence on properties of polymer nanocomposites. *Surf Interfaces.* 2021;22:100879. doi:[10.1016/j.surf.2020.100879](https://doi.org/10.1016/j.surf.2020.100879)
- Papanicolaou GC, Theocaris PS, Spathis GD. Adhesion efficiency between phases in fibre-reinforced polymers by means of the concept of boundary interphase. *Colloid Polym Sci.* 1980;258:1231–1237. doi:[10.1007/BF01668768](https://doi.org/10.1007/BF01668768)
- Alimardani M, Razzaghi-Kashani M, Ghoreishy MH. Prediction of mechanical and fracture properties of rubber composites by microstructural modeling of polymer-filler interfacial effects. *Mater Des.* 2017;115:348–354. doi:[10.1016/j.matdes.2016.11.061](https://doi.org/10.1016/j.matdes.2016.11.061)
- Nilagiri Balasubramanian KB, Ramesh T. Role, effect, and influences of micro and nano-fillers on various properties of polymer matrix composites for microelectronics: a review. *Polym Adv Technol.* 2018;29:1568–1585. doi:[10.1002/pat.4280](https://doi.org/10.1002/pat.4280)
- Ahmad Z, Sarwar MI, Mark JE. Thermal and mechanical properties of aramid-based titania hybrid composites. *J Appl Polym Sci.* 1998;70:297–302. doi:[10.1002/\(SICI\)1097-4628\(19981010\)70:2<297::AID-APP9>3.0.CO;2-P](https://doi.org/10.1002/(SICI)1097-4628(19981010)70:2<297::AID-APP9>3.0.CO;2-P)
- Laura DM, Keskkula H, Barlow JW, Paul DR. Effect of glass fiber and maleated ethylene-propylene rubber content on tensile and impact properties of Nylon 6. *Polymer.* 2000;41:7165–7174. doi:[10.1016/S0032-3861\(00\)00049-5](https://doi.org/10.1016/S0032-3861(00)00049-5)
- Alsewailam FD, Gupta RK. Effect of impact modifier types on mechanical properties of rubber-toughened glass-fibre-reinforced nylon 66. *Can J Chem Eng.* 2006;84:693–703. doi:[10.1002/cjce.5450840608](https://doi.org/10.1002/cjce.5450840608)
- Aliotta L, Cinelli P, Coltelli MB, Lazzeri A. Rigid filler toughening in PLA-Calcium Carbonate composites: Effect of particle surface treatment and matrix plasticization. *Eur Polym J.* 2019;113:78–88. doi:[10.1016/j.eurpolymj.2018.12.042](https://doi.org/10.1016/j.eurpolymj.2018.12.042)
- Sun R, Melton M, Safaie N, Ferrier Jr RC, Cheng S, Liu Y, Zuo X, Wang Y. Molecular view on mechanical reinforcement in polymer nanocomposites. *Phys Rev Lett.* 2021;126:117801. doi:[10.1103/PhysRevLett.126.117801](https://doi.org/10.1103/PhysRevLett.126.117801)
- Kishore K, Pandey A, Wagri NK, Saxena A, Patel J, Al-Fakih A. Technological challenges in nanoparticle-modified geopolymer concrete: A comprehensive review on nanomaterial dis-

- persion, characterization techniques and its mechanical properties. *Case Stud Constr Mater.* 2023;19:e02265. doi:[10.1016/j.cscm.2023.e02265](https://doi.org/10.1016/j.cscm.2023.e02265)
28. Jagadeesh P, Puttegowda M, Mavinkere Rangappa S, Siengchin S. Influence of nanofillers on biodegradable composites: A comprehensive review. *Polym Compos.* 2021;42:5691–5711. doi:[10.1002/pc.26291](https://doi.org/10.1002/pc.26291)
29. Mozetič M. Surface modification to improve properties of materials. *Mater.* 2019;12:441. doi:[10.3390/ma12030441](https://doi.org/10.3390/ma12030441)
30. Ersoy O, Köse H. Comparison of the effect of reactive and nonreactive treatments on the dispersion characteristics of a calcium carbonate (calcite) filler in a polypropylene matrix composite. *Polym Compos.* 2020;41:3483–3490. doi:[10.1002/pc.25634](https://doi.org/10.1002/pc.25634)
31. Patti A, Lecocq H, Serghei A, Acierno D, Cassagnau P. The universal usefulness of stearic acid as surface modifier: applications to the polymer formulations and composite processing. *J Ind Eng Chem.* 2021;96:1–33. doi:[10.1016/j.jiec.2021.01.024](https://doi.org/10.1016/j.jiec.2021.01.024)
32. Owuamanam S, Cree D. Progress of bio-calcium carbonate waste eggshell and seashell fillers in polymer composites: a review. *J Compos Sci.* 2020;4:70. doi:[10.3390/jcs4020070](https://doi.org/10.3390/jcs4020070)
33. Praveenkumara J, Madhu P, Yashas Gowda TG, Sanjay MR, Siengchin S. A comprehensive review on the effect of synthetic filler materials on fiber-reinforced hybrid polymer composites. *J Text I.* 2022;113:1231–1239. doi:[10.1080/00405000.2021.1920151](https://doi.org/10.1080/00405000.2021.1920151)
34. Ouyang Y, Bai L, Tian H, Li X, Yuan F. Recent progress of thermal conductive polymer composites: Al₂O₃ fillers, properties and applications. *Compos Part A Appl Sci Manufact.* 2022;152:106685. doi:[10.1016/j.compositesa.2021.106685](https://doi.org/10.1016/j.compositesa.2021.106685)
35. Kumar A, Sharma K, Dixit AR. A review on the mechanical properties of polymer composites reinforced by carbon nanotubes and graphene. *Carbon Lett.* 2021;31:149–165. doi:[10.1007/s42823-020-00161-x](https://doi.org/10.1007/s42823-020-00161-x)
36. Sharma M, Sharma R, Sharma SC. A review on fibres and fillers on improving the mechanical behaviour of fibre reinforced polymer composites. *Mater Today Proc.* 2021;46:6482–6489. doi:[10.1016/j.matpr.2021.03.667](https://doi.org/10.1016/j.matpr.2021.03.667)
37. Aziz T, Ullah A, Fan H, Jamil MI, Khan FU, Ullah R, Iqbal M, Ali A, Ullah B. Recent progress in silane coupling agent with its emerging applications. *J Polym Environ.* 2021;1:1–7. doi:[10.1007/s10924-021-02142-1](https://doi.org/10.1007/s10924-021-02142-1)
38. Zhang Y, Ding C, Zhang N, Chen C, Di X, Zhang Y. Surface modification of silica micro-powder by titanate coupling agent and its utilization in PVC based composite. *Constr Build Mater.* 2021;307:124933. doi:[10.1016/j.conbuildmat.2021.124933](https://doi.org/10.1016/j.conbuildmat.2021.124933)
39. Boufassa S, Hellati A, Doufnoune R. Correlations between the mechanical and thermal properties of polypropylene/high density polyethylene/CaCO₃ composites with the presence of coupling agents. *Rev Roum Chim.* 2019;64:1073–1082. doi:[10.33224/rrch.2019.64.12.07](https://doi.org/10.33224/rrch.2019.64.12.07)
40. Kusuktham B. Mechanical properties and morphologies of high density polyethylene reinforced with calcium carbonate and sawdust compatibilized with vinyltriethoxysilane. *Silicon.* 2019;11:1997–2013. doi:[10.1007/s12633-018-0020-0](https://doi.org/10.1007/s12633-018-0020-0)
41. Ming Y, Zhou Z, Hao T, Nie Y. Polymer Nanocomposites: Role of modified filler content and interfacial interaction on crystallization. *Eur Polym J.* 2022;162:110894. doi:[10.1016/j.eurpolymj.2021.110894](https://doi.org/10.1016/j.eurpolymj.2021.110894)
42. Li G, Zhao T, Zhu P, He Y, Sun R, Lu D, Wong CP. Structure-property relationships between microscopic filler surface chemistry and macroscopic rheological, thermo-mechanical, and adhesive performance of SiO₂ filled nanocomposite underfills. *Compos Part A Appl Sci Manufact.* 2019;118:223–234. doi:[10.1016/j.compositesa.2018.12.008](https://doi.org/10.1016/j.compositesa.2018.12.008)
43. Huang L, Yu F, Liu Y, Lu A, Song Z, Liu W, Xiong Y, He H, Li S, Zhao X, Cui S. Understanding the reinforcement effect of fumed silica on silicone rubber: Bound rubber and its entanglement network. *Macromolec.* 2022;56:323–334. doi:[10.1021/acs.macromol.2c01969](https://doi.org/10.1021/acs.macromol.2c01969)
44. Wagner MP. Reinforcing silicas and silicates. *Rubber Chem Technol.* 1976;49:703–774. doi:[10.5254/1.3534979](https://doi.org/10.5254/1.3534979)
45. Muhammad AM, Gupta NK. Nanostructured SiO₂ material: synthesis advances and applications in rubber reinforcement. *RSC Adv.* 2022;12:18524–18546. doi:[10.1039/D2RA02747J](https://doi.org/10.1039/D2RA02747J)
46. Maldas D, Kokta BV, Raj RG, Daneault C. Improvement of the mechanical properties of sawdust wood fibre–polystyrene composites by chemical treatment. *Polymer.* 1988;29:1255–1265. doi:[10.1016/0032-3861\(88\)90053-5](https://doi.org/10.1016/0032-3861(88)90053-5)
47. Zhang Y, Ding C, Zhang N, Chen C, Di X, Zhang Y. Surface modification of silica micro-powder by titanate coupling agent and its utilization in PVC based composite. *Constr Build Mater.* 2021;307:124933. doi:[10.1016/j.conbuildmat.2021.124933](https://doi.org/10.1016/j.conbuildmat.2021.124933)
48. Bigg DM. Mechanical properties of particulate filled polymers. *Polym Compos.* 1987;8:115–122. doi:[10.1002/pc.750080208](https://doi.org/10.1002/pc.750080208)
49. Ananthapadmanabha GS, Deshpande V. Influence of aspect ratio of fillers on the properties of acrylonitrile butadiene styrene composites. *J Appl Polym Sci.* 2018;135:46023. doi:[10.1002/app.46023](https://doi.org/10.1002/app.46023)
50. Fu SY, Feng XQ, Lauke B, Mai YW. Effects of particle size, particle/matrix interface adhesion and particle loading on mechanical properties of particulate–polymer composites. *Compos Part B Eng.* 2008;39:933–961. doi:[10.1016/j.compositesb.2008.01.002](https://doi.org/10.1016/j.compositesb.2008.01.002)
51. Leong YW, Abu Bakar MB, Ishak ZM, Ariffin A, Pukanszky B. Comparison of the mechanical properties and interfacial interactions between talc, kaolin, and calcium carbonate filled polypropylene composites. *J Appl Polym Sci.* 2004;91:3315–3326. doi:[10.1002/app.13542](https://doi.org/10.1002/app.13542)
52. Tian Q, Yuan Q, Fang L, Wang Y, Liu Z, Deng D. Estimation of elastic modulus of cement asphalt binder with high content of asphalt. *Constr Build Mater.* 2017;133:98–106. doi:[10.1016/j.conbuildmat.2016.12.003](https://doi.org/10.1016/j.conbuildmat.2016.12.003)
53. Madani M. Mechanical properties of polypropylene filled with electron beam modified surface-treated titanium dioxide nanoparticles. *J Reinf Plast Compos.* 2010;29:1999–2014. doi:[10.1177/0731684409341089](https://doi.org/10.1177/0731684409341089)
54. Cazan C, Enesca A, Andronic L. Synergic effect of TiO₂ filler on the mechanical properties of polymer nanocomposites. *Polymers.* 2021;13:2017. doi:[10.3390/polym13122017](https://doi.org/10.3390/polym13122017)
55. Nielsen LE. Simple theory of stress-strain properties of filled polymers. *J Appl Polym Sci.* 1966;10:97–103. doi:[10.1002/app.1966.070100107](https://doi.org/10.1002/app.1966.070100107)